

Numerical Investigation of Mixed Convection Flow of Viscoelastic Nanofluid with Convective Conditions over an Exponentially Stretching Surface

Bilal, Ashraf Mohammad*⁺

Department of Mathematics, COMSATS University Islamabad, Islamabad Campus, Islamabad, PAKISTAN

Mabood, Fazle

Department of Information Technology, Fanshawe College London, London, ON, CANADA

ABSTRACT: Numerical analysis is performed for a 3D incompressible viscoelastic nanofluid mixed convection flow model under the implications of convective boundary conditions towards an exponentially stretching sheet. The system that comprises differential equations of partial derivatives is remodeled into the system of differential equations via similarity transformations and then solved numerically through the Runge-Kutta-Fehlberg with shooting technique. The physical parameters, which emerge from the derived system are discussed in graphical formats. The significant outcomes of the current investigation are that the velocity field grows for a higher viscoelastic parameter while it reduces the fluid temperature. An increase in the mixed convection parameter diminishes the temperature and concentration. Further, the heat transfer rate is crumbled with the incremental values of the viscoelastic parameter. The obtained results show a better agreement with those available in the literature for limiting scenarios.

KEYWORDS: Viscoelastic fluid; 3D-flow; Mixed convection; Convective boundary conditions; Streamlines.

INTRODUCTION

Much deliberation in the inscription has been specified to the streams by a straight stretching surface. Nevertheless, this appears not practical when the procedures for plastic and polymer expulsion are thought of. In these dealings extending velocity is nonlinear. Extremely less consideration is given to the streams produced by power-law extending velocities. Mgyari and Keller [1] investigated the flow behavior and heat transfer due to the exponentially stretching of a surface with an exponential temperature distribution. Okechi *et al.* [2] presented the boundary layer analysis of flow-induced by rapidly stretching curved surfaces with exponential

velocity. An investigative arrangement of the nanofluid stream over an exponentially extending surface was introduced by Nadeem and Lee [3]. Warmth move examination over an exponentially contracting surface through the shooting technique was researched by Bhattacharyya [4]. Numerical study of non-Newtonian fluid flow over an exponentially stretching surface: an optimal HAM validation was studied by Rehman *et al.* [5]. Double diffusive mixed convection flow from a vertical exponentially stretching surface in presence of the viscous dissipation was provided by Patil *et al.* [6]. The three-dimensional progression of thick liquid over an exponentially

* To whom correspondence should be addressed.

+ E-mail: bilalashraf_gau@yahoo.com

1021-9986/2021/6/1931-1942

12/\$/6.02

extending surface with heat move was concentrated by *Liu et al.* [7]. *Hayat et al.* [8] extended the work of *Liu et al.* [7] for viscoelastic fluid in the presence of thermal radiation and mixed convection effects.

Mabood et al. [9] deal with the magnetohydrodynamic flow and heat transfer over a permeable stretching sheet via the Homotopy Analysis Method (HAM). The effect of thermal radiation is included in the energy equation, while velocity and thermal slips are included in the boundary conditions. *Mabood et al.* [10] analyzed the hydromagnetic mixed convective flow with heat and mass transfer over a vertical plate embedded in a porous medium, they observed that the rate of heat transfer decreases with increased values of magnetic and slips parameters, *Motsa et al.* [11] tended to the progression of upper convected Maxwell liquid over a permeable extending sheet within the sight of a magnetic field.

Nanofluids have been proposed as a means for enhancing the performance of heat transfer liquids currently available, such as water, toluene, oil, and ethylene glycol mixture. Initially, the nanofluid term is used by *Choi and Eastman* [12]. *Sheikholeslami et al.* [13] presented a Control Volume-based Finite Element Method (CVFEM) on nanofluid radiative heat transfer analysis in a porous medium using Darcy Model, where they observed that the rise in Hatmann number reduce the Average Nusselt number while the radiation parameter uplifts it. *Sheikholeslami et al.* [14] introduced a new computational scheme for the exergy and entropy analysis of nanofluid in a porous medium, *Hayat et al.* [15] provided the study of Casson nanofluid over a stretching surface in presence of thermal radiation, heat source/sink, and first-order chemical reaction. *Sheikholeslami and Ganji* [16] examined the warmth move of Cu-water nanofluid streams between equal plates. *Turkyilmazoglu* [17] analyzed the flimsy blended convection stream of nanofluid over a moving vertical level plate with heat move. *Ashraf et al.* [18] tended to the three-dimensional progression of an Eyring-Powell nanofluid with convective limit conditions over an exponentially extending surface. After that mixed convection flow of magnetohydrodynamic (MHD) Jeffrey, nanofluid over a radially stretching surface with the radiative surface was discussed by *Ashraf et al.* [19]. *Mabood et al.* [20] investigated the heat generation/absorption and chemical reaction on a non-Newtonian (Sisko) nanofluid over

a stretching surface under the influence of nonlinear radiation. *Mabood and Das* [21] presented the melting heat transfer of a nanofluid over a stretching surface taking into account a second-order slip model and thermal radiation. *Mabood et al.* [22] reported the combined effects of the chemical reaction and viscous dissipation on MHD radiative heat and mass transfer of nanofluid flow over a rotating stretching surface. *Sheikholeslami and Sadoughi* [23] detailed nanofluid convective stream within the sight of a liquefying surface. Nanofluid conduct in the presence of Coulomb force was shown by *Sheikholeslami and Chamkha* [2]. Some interesting features of nanofluids and heat transfer analysis can be found in Refs. [25-32].

Ashraf et al. [33] provided the mixed convection radiative flow of three-dimensional Maxwell fluid over an inclined stretching sheet in the presence of thermophoresis and convective condition. Soret and Dufour effects on the mixed convection flow of an Oldroyd-B fluid with convective boundary conditions was studied by *Ashraf et al.* [34]. *Turkyilmazoglu* [35] talked about the blended convection stream over a porous extending surface, where the author reported that the existence of unique or double solutions strongly relies on the Prandtl number, *Mabood et al.* [36] presented the heat transfer of micropolar fluid in the presence of binary chemical reaction and Arrhenius activation energy, it is mentioned that flow is undermined due to viscosity and buoyancy parameters which establishing the wider velocity boundary layer. *Ashraf et al.* [37] provided the mixed convection flow of Casson fluid over a stretching sheet with convective boundary conditions and Hall effect. Convective heat and mass transfer in the presence of chemical reaction and heat source/sink were studied by *Ashraf et al.* [38]. *Sheikholeslami et al.* [39] provided the magnetohydrodynamic nanofluid flow and convective heat transfer in a porous cavity.

From the aforementioned literature, the mixed convection viscoelastic nanofluid 3D flow with convective boundary conditions is not studied yet, to fill this gap, we examine the mixed convection flow of viscoelastic nanofluid with convective boundary conditions for heat and mass transfer over the exponentially stretching surface. Similarity transformations are utilized to reduce the partial differential equations into the ordinary differential equations. The resulting boundary layer system is solved by using Runge-Kutta-Fehlberg [40].

A variety of all the physical boundaries engaged with

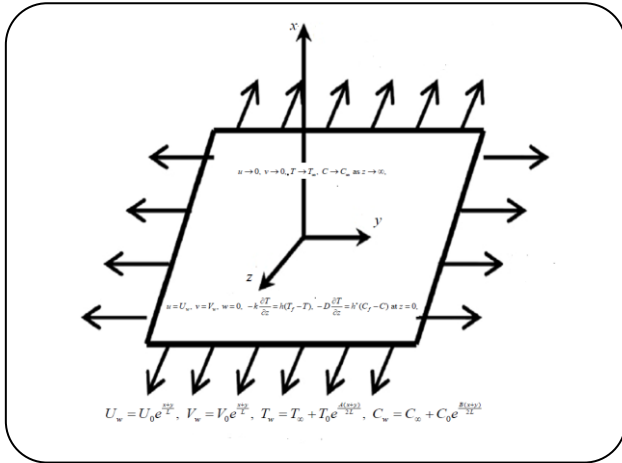


Fig. A: Physical Problem.

the flow problem is analyzed for the flow field, temperature, and concentration.

THEORETICAL SECTION

Mathematical modeling

We talk about the blended convection limit layer stream of viscoelastic nanofluid over an exponentially extending surface. The surface agrees with the plane at $z=0$ and the stream is limited in the area $z>0$, as shown in Fig A.

Convective limit conditions for both warmth and mass exchange on the outside of a sheet are picked. The overseeing limit layer conditions for three-dimensional streams can be placed into the forms [18]:

$$\frac{\partial u}{\partial x} + \frac{\partial v}{\partial y} + \frac{\partial w}{\partial z} = 0 \tag{1}$$

$$u \frac{\partial u}{\partial x} + v \frac{\partial u}{\partial y} + w \frac{\partial u}{\partial z} = v \frac{\partial^2 u}{\partial z^2} + \left(\frac{\partial u}{\partial x} \frac{\partial^2 u}{\partial z^2} + \frac{\partial u}{\partial z} \frac{\partial^2 w}{\partial z^2} + 2 \frac{\partial u}{\partial z} \frac{\partial^2 u}{\partial x \partial z} + 2 \frac{\partial w}{\partial z} \frac{\partial^2 u}{\partial z^2} \right) + g \beta_T (T - T_\infty) + g \beta_C (C - C_\infty) \tag{2}$$

$$g \beta_T (T - T_\infty) + g \beta_C (C - C_\infty) \tag{3}$$

$$u \frac{\partial v}{\partial x} + v \frac{\partial v}{\partial y} + w \frac{\partial v}{\partial z} = v \frac{\partial^2 v}{\partial z^2} + \left(\frac{\partial v}{\partial y} \frac{\partial^2 v}{\partial z^2} + \frac{\partial v}{\partial z} \frac{\partial^2 w}{\partial z^2} + 2 \frac{\partial v}{\partial z} \frac{\partial^2 v}{\partial y \partial z} + 2 \frac{\partial w}{\partial z} \frac{\partial^2 v}{\partial z^2} \right) \tag{3}$$

$$\frac{k_0}{\rho} \left[v \frac{\partial^3 v}{\partial y \partial z^2} + w \frac{\partial^3 v}{\partial z^3} - \left(\frac{\partial v}{\partial y} \frac{\partial^2 v}{\partial z^2} + \frac{\partial v}{\partial z} \frac{\partial^2 w}{\partial z^2} + 2 \frac{\partial v}{\partial z} \frac{\partial^2 v}{\partial y \partial z} + 2 \frac{\partial w}{\partial z} \frac{\partial^2 v}{\partial z^2} \right) \right] \tag{3}$$

$$u \frac{\partial T}{\partial x} + v \frac{\partial T}{\partial y} + w \frac{\partial T}{\partial z} = \sigma \frac{\partial^2 T}{\partial z^2} + \left(\frac{\partial u}{\partial x} \frac{\partial T}{\partial z} + \frac{\partial v}{\partial y} \frac{\partial T}{\partial z} + \frac{D_T}{T_\infty} \left(\frac{\partial T}{\partial z} \right)^2 \right) \tag{4}$$

$$\frac{\rho^* c_p^*}{\rho c_p} \left(D_B \frac{\partial C}{\partial z} \frac{\partial T}{\partial z} + \frac{D_T}{T_\infty} \left(\frac{\partial T}{\partial z} \right)^2 \right) \tag{4}$$

$$u \frac{\partial C}{\partial x} + v \frac{\partial C}{\partial y} + w \frac{\partial C}{\partial z} = D_B \frac{\partial^2 C}{\partial z^2} + \frac{D_T}{T_\infty} \frac{\partial^2 T}{\partial z^2} \tag{5}$$

Where the above conditions and $u, v,$ and w are the velocity parts in the $x-, y-$ and $z-$ directions respectively, k_0 material liquid parameter, β_T warm extension coefficient, concentration development coefficient, D_B mass diffusivity, ρ^* density of nanoparticles, c_p^* specific heat of nanoparticles and prime denotes the differentiation with respect to η .

The boundary conditions can be expressed as follows:

$$u = U_w, v = V_w, w = 0, -k \frac{\partial T}{\partial z} = h(T_f - T), \tag{6}$$

$$-D \frac{\partial T}{\partial z} = h^*(C_f - C) \text{ at } z = 0,$$

$$u \rightarrow 0, v \rightarrow 0, T \rightarrow T_\infty, C \rightarrow C_\infty \text{ as } z \rightarrow \infty \tag{7}$$

$$U_w = U_0 e^{\frac{x+y}{L}}, V_w = V_0 e^{\frac{x+y}{L}}, T_w = T_\infty + T_0 e^{\frac{A(x+y)}{2L}}, \tag{8}$$

$$C_w = C_\infty + C_0 e^{\frac{B(x+y)}{2L}},$$

By using the transformations [7]:

$$u = U_0 e^{\frac{x+y}{L}} f'(\eta), v = U_0 e^{\frac{x+y}{L}} g'(\eta), \tag{9}$$

$$w = - \left(\frac{v U_0}{2L} \right)^{1/2} e^{\frac{x+y}{2L}} (f + \eta f' + g + \eta g'),$$

$$T = T_\infty + T_0 e^{\frac{A(x+y)}{2L}} \theta(\eta), C = C_\infty + C_0 e^{\frac{B(x+y)}{2L}} \phi(\eta),$$

$$\eta = \left(\frac{U_0}{2vL} \right)^{1/2} e^{\frac{x+y}{2L}} z$$

Eq. (1) is identically fulfilled and Eqs. (2)-(9) give:

$$f''' + (f + g)f'' - 2(f' + g')f' + \left(6f'''f' + (3g'' - 3f'' + \eta g''')f'' + ((4g' + 2\eta g'')f''' - (f + g + \eta g')f'''' \right) + 2\lambda(\theta + N_r \phi) = 0, \tag{10}$$

$$g''' + (f + g)g'' - 2(f' + g')g' + \quad (11)$$

$$K \left(\begin{array}{l} 6g'''g' + (3f'' - 3g'' + \eta f''')g'' \\ + (4f' + 2\eta f'')g''' - (f + g + \eta f')g'''' \end{array} \right) = 0$$

$$\theta'' + Pr(f + g)\theta' - PrA(f' + g')\theta + \quad (12)$$

$$(N_b\theta'\phi' + N_t\theta'^2) = 0$$

$$\phi'' + Sc(f + g)\phi' - ScA(f' + g')\phi + \frac{N_t}{N_b}\theta'' = 0 \quad (13)$$

$$f = 0, \quad g = 0, \quad f' = 1, \quad g' = \alpha, \quad \theta' = -\gamma_1(1 - \theta(0)), \quad (14)$$

$$\phi' = -\gamma_2(1 - \phi(0)), \quad \text{at } \eta = 0$$

$$f' \rightarrow 0, \quad g' \rightarrow 0, \quad \theta \rightarrow 0, \quad \phi \rightarrow 0 \quad \text{as } \eta \rightarrow \infty \quad (15)$$

Where K viscoelastic parameter, λ mixed convection parameter, Gr_x local Grashof number, N_r concentration buoyancy parameter, Pr Prandtl number, Sc Schmidt number, α ratio parameter, γ_1 heat transfer Biot number and γ_2 mass transfer Biot number. These can be defined in the forms:

$$K = \frac{k_0 U_w}{2\nu L}, \quad \lambda = \frac{Gr_x}{Re_x^2}, \quad Gr_x = \frac{g\beta_T(T_f - T_\infty)x^3}{\nu^2}, \quad (16)$$

$$N_r = \frac{\beta_C(C_w - C_\infty)}{\beta_T(T_f - T_\infty)}, \quad Pr = \frac{\nu}{\sigma}, \quad Sc = \frac{\nu}{D}, \quad \alpha = \frac{V_0}{U_0},$$

$$\gamma_1 = \frac{h}{k} \sqrt{\frac{\nu}{a}}, \quad \gamma_2 = \frac{h^*}{D} \sqrt{\frac{\nu}{a}}$$

The heat transfer at wall and mass transfer at wall numbers in dimensionless forms can be expressed as follows:

$$Nu / Re_x^{1/2} = -\frac{x}{2L} \theta'(0) \quad (17)$$

$$Sh / Re_x^{1/2} = -\frac{x}{2L} \phi'(0), \quad (18)$$

where $Re_x = \frac{U_0 L}{\nu} e^{\frac{x+y}{L}}$ is the local Reynold number.

Numerical solution

The diminished conditions (10)- (15) are exceptionally non-direct and coupled and unraveled numerically utilizing Runge–Kutta–Fehlberg (RKF) with shooting

technique for various estimations of boundaries. The effect of the different boundaries on the speed, temperature, concentration, warmth, and mass exchange rates are concentrated graphically. The step size is taken $\Delta\eta = 0.01$ furthermore, precision is up to the fifth decimal spot as the measure of combination. We expected an appropriate limited an incentive for the far-field boundary condition in (15), i.e. $\eta \rightarrow \infty$, say η_∞ .

$$f'(\eta_{max}) = g'(\eta_{max}) = \theta(\eta_{max}) = \phi(\eta_{max}) \rightarrow 0$$

Figs. 1(a-c) are drafted to evaluate the impressions of the viscoelastic parameter K , the mixed convection parameter λ and the concentration buoyancy parameter N_r on the velocity profile $f'(\eta)$. It is to be found from Fig. 1a that the velocity profile $f'(\eta)$ enhances with an increase in the viscoelastic parameter K . As viscoelastic parameter K is the ratio of wall velocity and kinematic viscosity. That's why as the viscoelastic parameter K enhances this means that the velocity of the fluid is more dominant than the viscosity of the fluid due to which velocity profile increases. It is to be depicted from Figs. 1b and 1c that within an increase in the mixed convection parameter λ and the concentration buoyancy parameter N_r the velocity profile $f'(\eta)$ increases. Figs. 2a-2c are sketched to discuss the impacts of ratio parameter α , temperature exponent A and heat transfer Biot number γ_1 on the velocity profile $f'(\eta)$. It is to be noted that the velocity profile and the momentum boundary layer thickness decrease within an enhancement in ratio parameter and temperature exponent A while the velocity profile and the momentum boundary layer thickness increase within an enhancement in heat transfer biot number γ_1 . Variations of the viscoelastic parameter K , ratio parameter α and the mixed convection parameter λ on the secondary velocity profile $g'(\eta)$ are drawn in Figs. 3a-3c. It is to be observed that with in an enhancement in viscoelastic parameter K and ratio parameter α both the secondary velocity profile $g'(\eta)$ and the momentum boundary layer thickness enhances. It is also seen that the impact of the mixed convection parameter λ on the secondary profile $g'(\eta)$ is decreasing.

The influence of the K , λ , and N_r on the temperature $\theta(\eta)$ are analyzed in Figs. 4a-4c. It is to be noted that both the thermal boundary layer thickness and temperature profile $\theta(\eta)$ decrease within an increase in K , λ and N_r . Thermal boundary layer thickness decreases with an

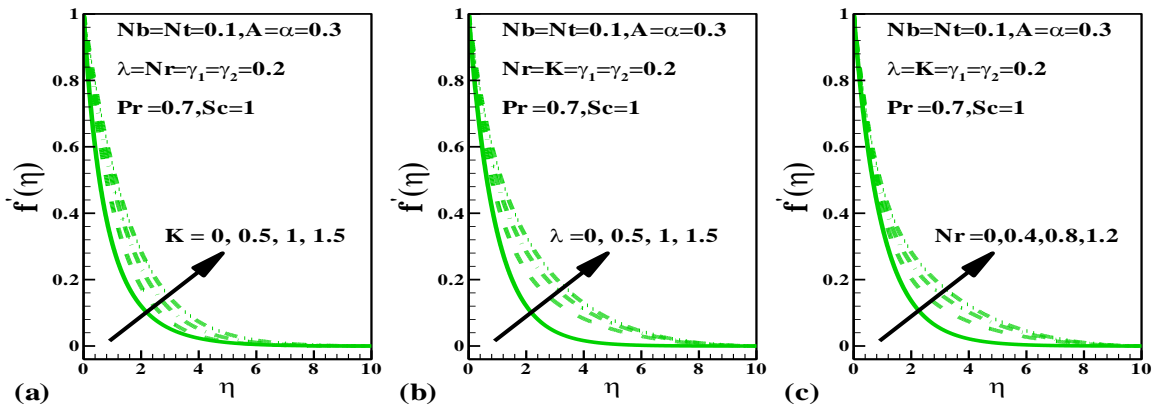


Fig. 1: Effect of K , Nr and λ on velocity.

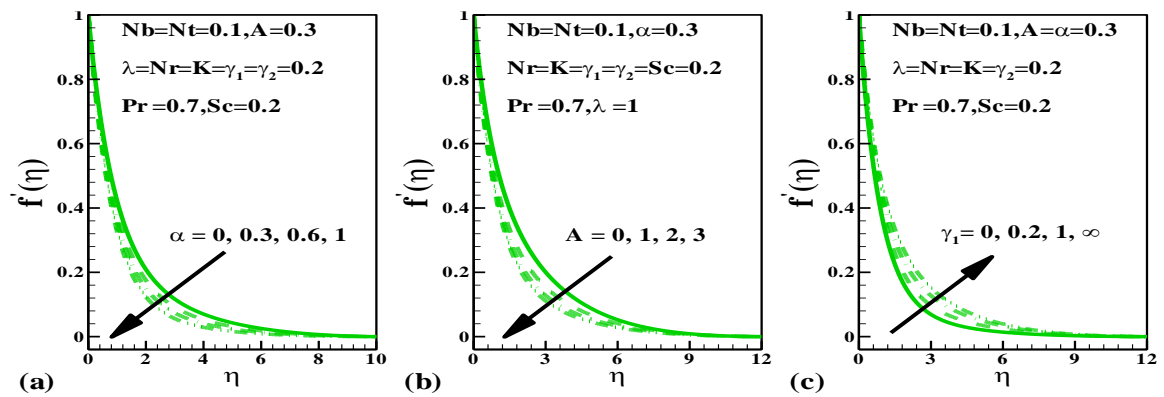


Fig. 2: Effect of α , A and γ on velocity.

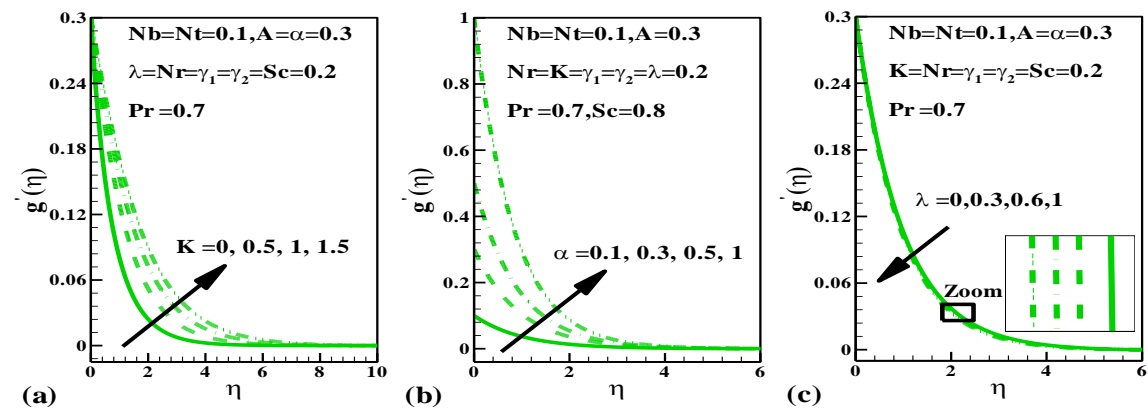


Fig. 3: Effect of K , α and λ on secondary velocity.

enhancement in ratio parameter α and temperature exponent A while enhancing within an increase in heat transfer biot number γ as seen in Figs. 5a-5c. Figs. 6a-6c are elucidated to discuss the impact of Prandtl number Pr , Brownian motion

parameter N_b , and thermophoresis parameter N_t on the temperature profile $\theta(\eta)$. It is noted that an increase in the Brownian motion parameter leads to an enhancement in the temperature $\theta(\eta)$ as well as the thermal boundary layer thickness.

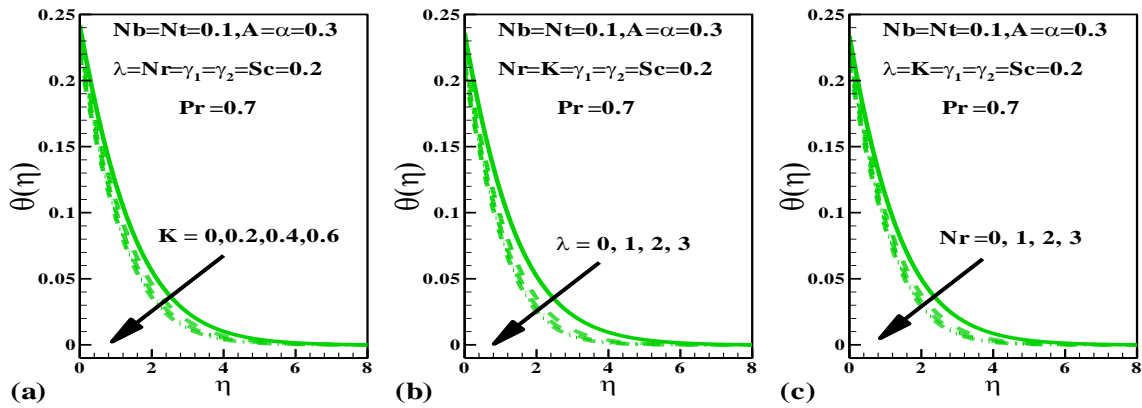


Fig. 4: Effect of K , Nr and λ on temperature.

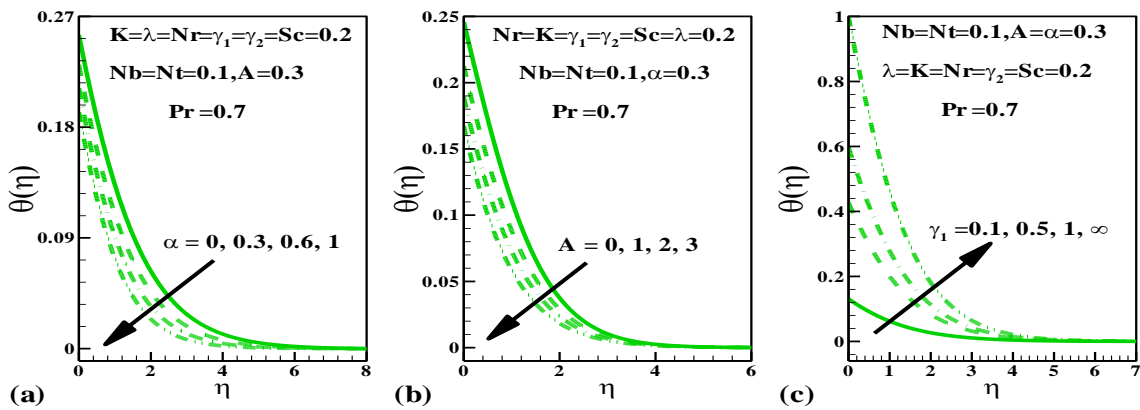


Fig. 5: Effect of α , A and γ_1 on temperature.

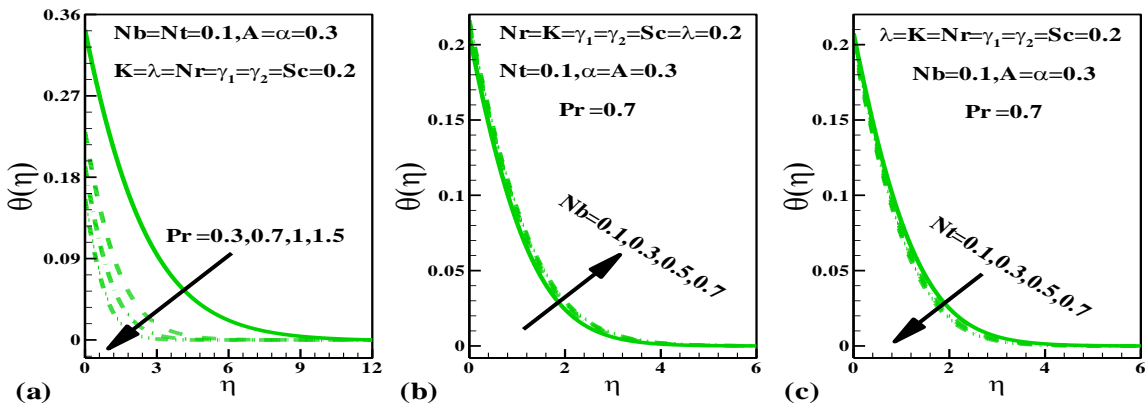


Fig. 6: Effect of Pr , B_b and N_t on temperature

Enhancement of thermophoresis parameters N_t and Pr reduces the thermal boundary layer thickness and the temperature $\theta(\eta)$. As Prandtl number Pr is the ratio of momentum diffusivity to thermal diffusivity which leads

to a decrease in both the thermal boundary layer thickness and the temperature $\theta(\eta)$ for increasing values of Pr .

Figs. 7-9 elucidates the variations of the K , λ , N_r , α , A , γ_1 , Sc , N_b and mass transfer Biot number γ_2 on the

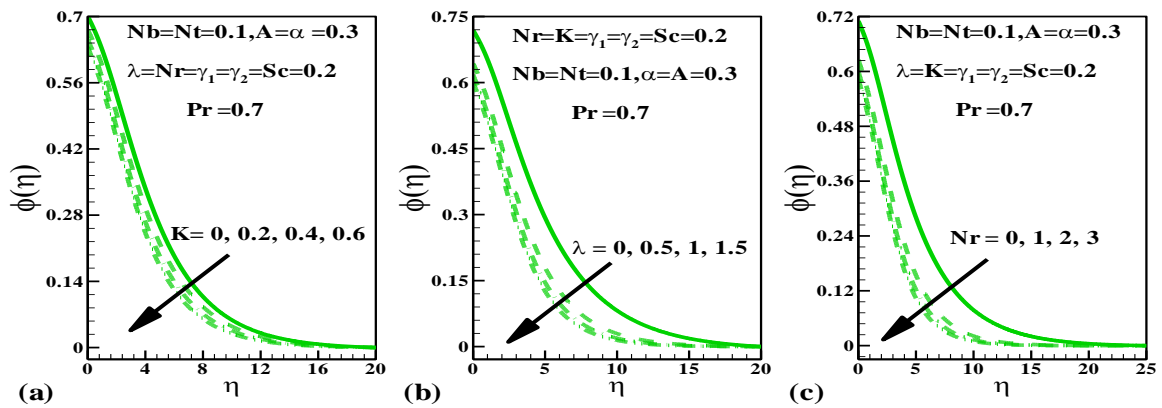


Fig. 7: Effect of K, λ and Nr on concentration.

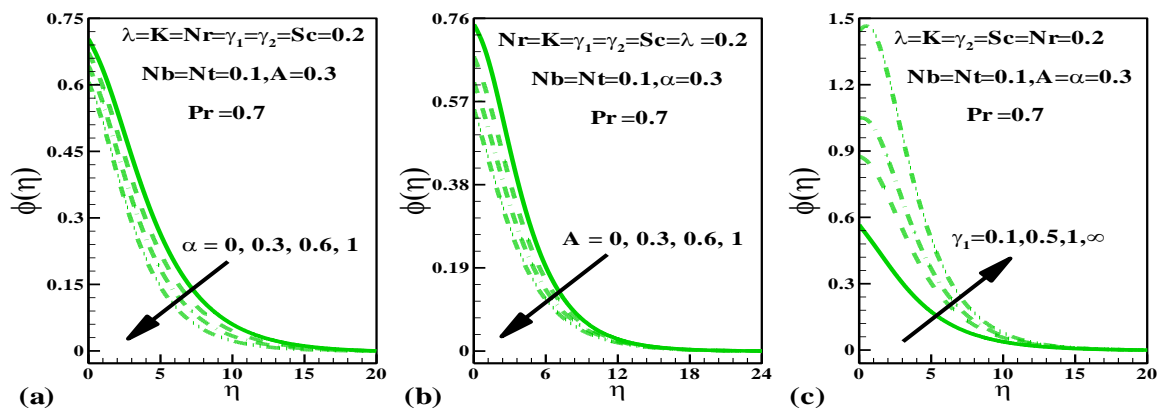


Fig. 8: Effect of α, A and γ_1 on concentration.

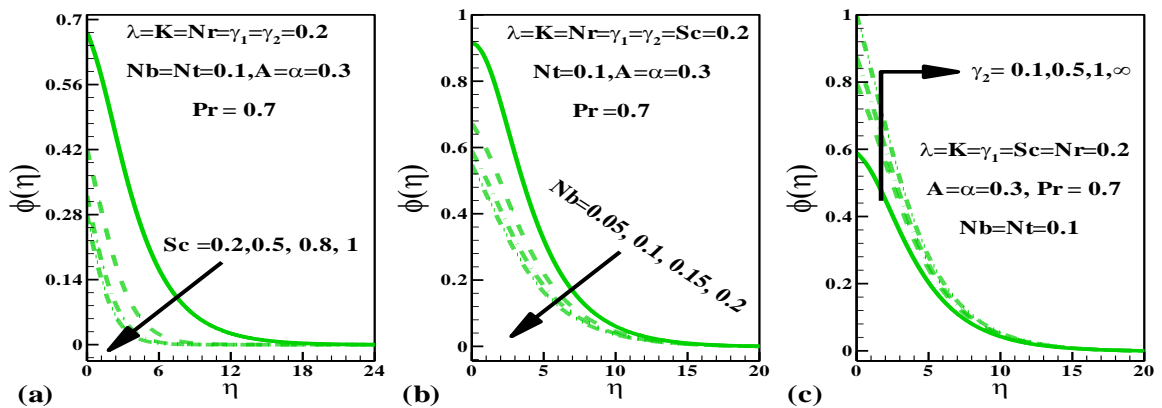


Fig. 9: Effect of Sc, Nb , and γ_2 on concentration.

concentration profile $\phi(\eta)$. From these Figures It is to be found that the concentration profile $\phi(\eta)$ and the associated boundary layer thickness decreases with an increase in $K, \lambda, Nr, \alpha, A, Sc$ and Brownian motion parameter N_b while an increasing

function of heat transfer biot number γ_1 and mass transfer Biot number γ_2 . Figs. 10a-10b are plotted to analyze the effect of viscoelastic parameter K , mixed convection parameter λ , the concentration buoyancy parameter N_r , ratio parameter α ,

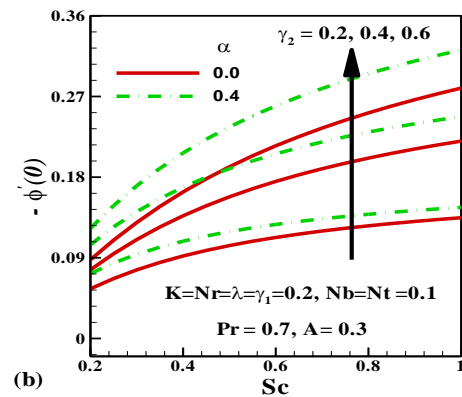
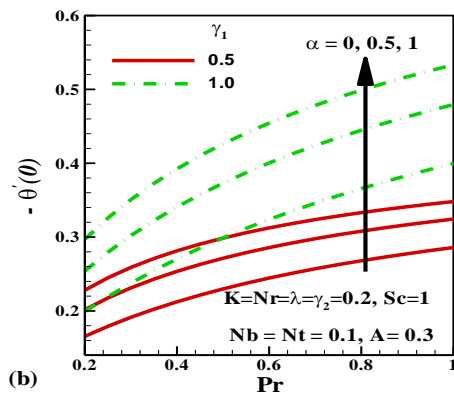
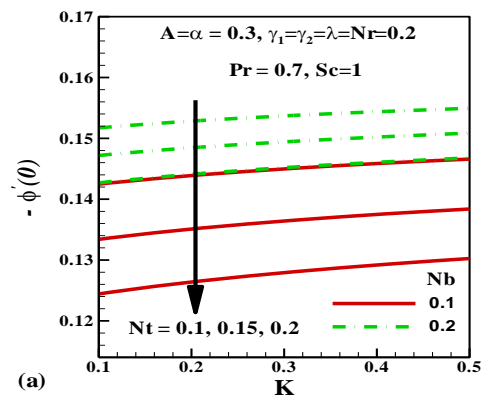
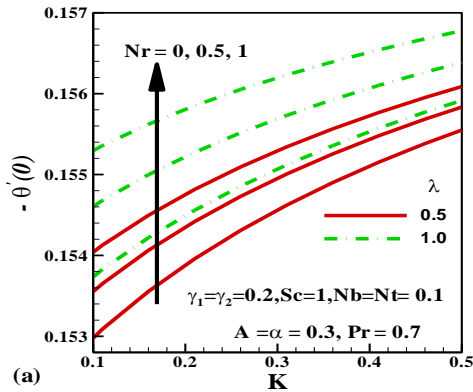


Fig. 10: Effect of K , λ , Nr & Pr , α , γ on Nusselt number.

Fig. 11: Effect of K , Nb , Nt & Sc , α , γ on Sherwood number.

temperature exponent A , and heat transfer Biot number γ_1 on the local Nusselt number $-\theta'(0)$. These figures show that the enhancement of the viscoelastic parameter K , mixed convection parameter λ , the concentration buoyancy parameter N_r , ratio parameter α and heat transfer Biot number γ_1 enhances the heat transfer at the wall $-\theta'(0)$. Figs. 11a-11b are drawn to see the impacts of physical quantities on the Sherwood number $-\phi'(0)$. It is to be noted that Sherwood number $-\phi'(0)$ is an increasing function of viscoelastic parameter K , mixed convection parameter λ , the concentration buoyancy parameter N_r , ratio parameter α , mass transfer Biot number γ_2 and Schmidt number Sc .

Tables 1 and 2 are computed to see the comparison of the numerical values of the physical quantities with the Hayat et al. [8] and Liu et al. [7]. Table 3 is computed to see the impacts of the viscoelastic parameter K , mixed convection parameter λ , the concentration buoyancy parameter N_r , ratio parameter α , temperature exponent A , Schmidt number Sc and Brownian motion parameter N_b

while an increasing function of heat transfer biot number γ_1 and mass transfer biot number γ_2 on the local Nusselt number $-\theta'(0)$ and the Sherwood number $-\phi'(0)$.

Fig. 12 represents the streamlines for different values of the viscoelastic parameter ($K= 0, 0.5, 1$). It is seen that the streamlines diverge more and more from the origin for rising K . Divergence upgrades for $K=0$ compared to that for $K=0.5, 1$. Figures 13 manifests the isotherms for different values of the viscoelastic parameter ($K= 0, 0.5, 1$). More isotherms converge at the origin as we hike K . At $K=0$, the convergence is low as compared with other values of K .

CONCLUSIONS

The main outcomes of the present study are as follows.

- Increment in K , λ and Nr leads to the escalation of flow field $f'(\eta)$ while that of α , A curtail it.
- Rise in K upsurges $g'(\eta)$ while that of λ peters out it.
- Thermal field $\alpha(\eta)$ and the related boundary layer thickness gets diminished with proper increment in K and α .

Table 1: Comparison of $-f''(0)$, $-g''(0)$ and $f(\infty)+g(\infty)$ when $K=\alpha = \lambda = A = \gamma_1 = 0$.

	$\alpha = 0$			$\alpha = 0.5$			$\alpha = 1$		
	[7]	[8]	Present	[7]	[8]	Present	[7]	[8]	Present
$-f''(0)$	1.28180856	1.28181	1.281816	1.56988846	1.56989	1.569889	1.81275105	1.81275	1.812754
$-g''(0)$	0	0	0	0.78494423	0.78494	0.784949	1.81275105	1.81275	1.812754
$f(\infty)+g(\infty)$	0.90564383	0.90564	0.902727	1.10918263	1.10918	1.108288	1.28077378	1.28077	1.280462

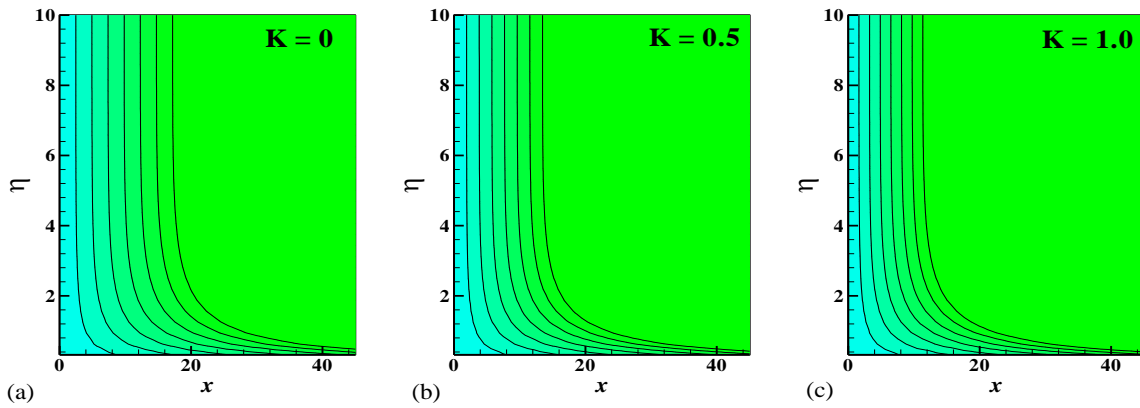


Fig. 12: Contour plots of streamlines for different values of K .

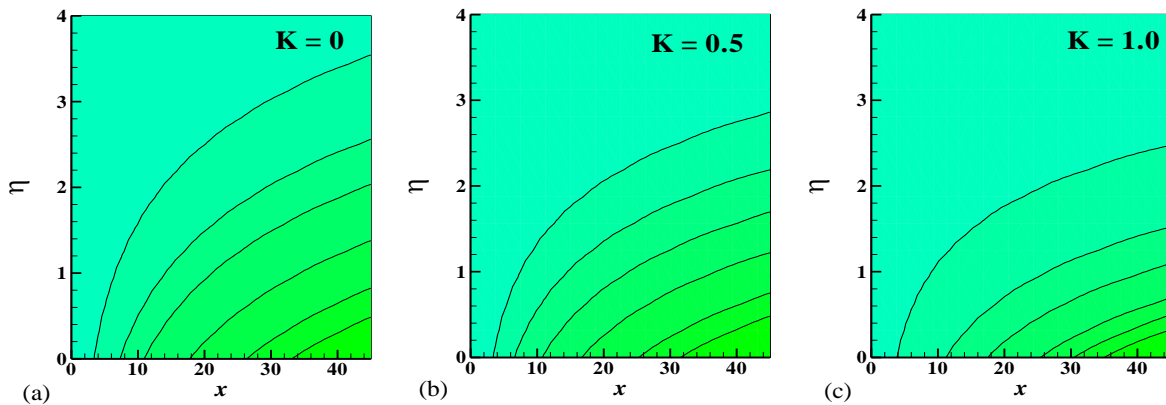


Fig. 13: Contour plots of isotherms for different values of K .

Table 2: Comparison of $-\theta'(0)$ when $K = 0.2$, $\alpha = \lambda = \gamma_1 = 0.5$, $Pr = 1.2$, $A = 0.2$.

Hayat et al. [8]	Present
0.329701	0.3297095754

- Augmented γ_1 yield escalated concentration field $\theta(\eta)$.
- Rise in K and Pr improves heat transfer rate from stretching surface.
- Streamlines/Isotherms diverge/converge more and more from/to an origin accordingly.

Table 3: Numerical values of Nusselt and Sherwood numbers for various values of parameters when $Pr = 0.7$, $Nb = Nt = 0.2$.

K	λ	Nr	α	A	γ_1	γ_2	Sc	$-\theta'(0)$	$-\phi(0)$
0.0	0.2	0.2	0.3	0.3	0.1	0.1	0.2	0.085975	0.053716
0.5								0.087456	0.058471
1.0								0.087994	0.061029
0.2	0.5							0.087083	0.057522
	1.0							0.087374	0.059067
	2.0							0.087754	0.060985
	0.3	0.4						0.087089	0.057652
		0.7						0.087275	0.058749
		1.0						0.087421	0.059578
		0.2	0.0					0.085339	0.053987
			0.5					0.087753	0.058289
			1.0					0.089333	0.061977
			0.3	0.2				0.086175	0.054783
				0.6				0.088659	0.061307
				1.0				0.090244	0.065999
				0.5	0.2			0.157620	0.077943
					0.5			0.299248	0.024101
					1.0			0.426495	0.003819
					0.2	0.3		0.157579	0.098819
						0.6		0.157503	0.135109
						1.0		0.157452	0.158478
						0.5	0.5	0.156736	0.225039
							0.8	0.156481	0.274162
							1.5	0.156362	0.330229

Received : Apr. 21, 2020 ; Accepted : July 13, 2020

REFERENCES

- [1] Magyari E., Keller B., Heat and Mass Transfer in the Boundary Layer on an Exponentially Stretching Continuous Surface, *J. Phys. D. Appl. Phys.*, **32**: 577-585 (1999).
- [2] Okechi N.F., Jamil M., Asghar S., Flow of Viscous Fluid Along an Exponentially Stretching Curved Surface, *Results in Physics*, **7**: 2851-2854 (2017).
- [3] Nadeem S., Lee C., Boundary Layer Flow of Nanofluid over an Exponentially Stretching Surface, *Nanoscale Research Letters*, **7**: 94 (2012).
- [4] Bhattacharyya K., Uddin M.S., Layek G.C., Malek M.A., Effect of Chemically Reactive Solute Diffusion on Boundary Layer Flow Past a Stretching Surface with Suction or Blowing, *J. Math. Math. Sci.*, **25**: 41-48 (2010).
- [5] Rehman S., Haq R., Lee C., Nadeem S., Numerical Study of Non-Newtonian Fluid Flow over an Exponentially Stretching Surface: an Optimal HAM Validation, *J. Braz. Soc. Mech. Sci. Eng.*, **39**: 1589-1596 (2017).
- [6] Patil P.M., Latha D.N., Roy S., Momoniat E., Double Diffusive Mixed Convection Flow from a Vertical Exponentially Stretching Surface in Presence of the Viscous Dissipation, *Int. J. Heat. Mass. Tran.*, **112**: 758-766 (2017).

- [7] Liu I.C., Wang H.H., Peng Y.F., Flow and Heat Transfer for Three Dimensional Flow over an Exponentially Stretching Surface, *Chem. Eng. Commun.*, **200**: 253-268 (2013).
- [8] Hayat T., Ashraf M.B., Alsulami H.H., Alhuthali M.S., Three Dimensional Mixed Convection Flow of Viscoelastic Fluid with Thermal Radiation and Convective Conditions, *Plos One*, **9**: e90038 (2014).
- [9] Mabood F., Nayak M.N., Chamkha A.J., Heat Transfer on the Cross Flow of Micropolar Fluids over a Thin Needle Moving in a Parallel Stream Influenced by Binary Chemical Reaction and Arrhenius Activation Energy, *The European Physical Journal Plus*, **134(9)**: 427 (2019).
- [10] Mabood F., Lorenzini G., Pochai N., Shateyi S., Homotopy Analysis Method for Radiation and Hydrodynamic-Thermal Slips Effects on MHD Flow and Heat Transfer Impinging on Stretching Sheet, *Defect and Diffusion Forum*, **388**: 317-327 (2018).
- [11] Motsa S.S., Hayat T., Aldossary O.M., MHD Flow of Upper- Convected Maxwell Fluid over Porous Stretching Sheet Using Successive Taylor Series Linearization Method, *Appl. Math. Mech.*, **33**: 975-990 (2012).
- [12] Choi S.U.S., Eastman J.A., Enhancing Thermal Conductivity of Fluids with Nanoparticles, *Materials Sci.*, **231**: 99-105 (1995).
- [13] Sheikholeslami M., Shahzad S.A., CVFEM Simulation for Nanofluid Migration in a Porous Medium Using Darcy Model, *Int. J. Heat Mass Transf.*, **122**: 1264-1271 (2018).
- [14] Sheikholeslami M., New Computational Approach for Exergy and Entropy Analysis of Nanofluid Under the Impact of Lorentz Force Through a Porous Media, *Computer Methods in Applied Mechanics and Engineering*, **344**: 319-333 (2019).
- [15] Hayat T., Bilal Ashraf M., Shehzad S.A., Alsaedi A., Mixed Convection Flow of Casson Nanofluid over a Stretching Sheet with Convectively Heated Chemical Reaction and Heat Source/Sink, *Journal of Applied Fluid Mechanics*, **8**: 803-813 (2015).
- [16] Sheikholeslami M., Ganji D.D., Heat Transfer of Cu-Water Nanofluid Flow Between Parallel Plates, *Powder Technology*, **235**: 873-879 (2013).
- [17] Turkyilmazoglu M., Unsteady Convection flow of Some Nanofluids Past a Moving Vertical flat Plate with Heat Transfer, *J. Heat Transf.* doi:10.1115/1.4025730.
- [18] Bilal Ashraf M., Hayat T., Alsaedi A., Three-Dimensional Flow of Eyring-Powell Nanofluid by Convectively Heated Exponentially Stretching Sheet, *Eur. Phys. J. Plus*, **130**: 5 (2015).
- [19] Bilal Ashraf M., Hayat T., Alsaedi A., Shehzad S.A., Convective Heat and Mass Transfer in MHD Mixed Convection Flow of Jeffrey Nanofluid over a Radially Stretching Surface with Thermal Radiation, *J. Cent. South Univ.*, **22**: 1114-1123 (2015).
- [20] Mabood F., Ibrahim S.M., Khan W.A., Effect of Melting and Heat Generation/Absorption on Sisko Nanofluid over a Stretching Surface with Nonlinear Radiation, *Physica Scripta*, **94(6)**: 065701 (2019).
- [21] Mabood F., Das K., Melting Heat Transfer on Hydro Magnetic Flow of a Nano Fluid over a Stretching Sheet with Radiation and Second-Order Slip, *Eur. Phys. J. Plus*, **131**: 3 (2016).
- [22] Mabood F., Ibrahim S.M., Khan W.A., Framing the Features of Brownian Motion and Thermophoresis on Radiative Nanofluid Flow Past a Rotating Stretching Sheet with Magnetohydrodynamics, *Results in Physics*, **6**: 1015-1023 (2016).
- [23] Sheikholeslami M., Sadoughi M.K., Simulation of CuO-Water Nanofluid Heat Transfer Enhancement in Presence of Melting Surface, *Int. J. Heat Mass Transf.*, **116**: 909-919 (2018).
- [24] Sheikholeslami M., Chamkha A.J., Electrohydrodynamic Free Convection Heat Transfer of a Nanofluid in a Semi-Annulus Enclosure with a Sinusoidal Wall, *Numer. Heat Transf. A*, **69(7)**: 781-793 (2016).
- [25] Sheikholeslami M., Rezaeianjouybari B., Darzi M., Shafee A., Li Z., Nguyen T. K., Application of Nano-Refrigerant for Boiling Heat Transfer Enhancement Employing an Experimental Study, *International Journal of Heat and Mass Transfer*, **141**: 974-980 (2019).
- [26] Sheikholeslami M., Haq R.ul., Shafee A., Li Z., Elaraki Y. G., Tlili I., Heat Transfer Simulation of Heat Storage Unit with Nanoparticles and Fins Through a Heat Exchanger, *International Journal of Heat and Mass Transfer*, **135**: 470-478 (2019).

- [27] Rezaeianjouybari B., Sheikholeslami M., Shafee A., Babazadeh H., A Novel Bayesian Optimization for Flow Condensation Enhancement Using Nanorefrigerant: a Combined Analytical and Experimental Study, *Chemical Engineering Science*, **215**: 115465 (2020).
- [28] Mahabaleshwar U.S., Sarris I.E., Lorenzini G., Effect of Radiation and Navier Slip Boundary of Walters' Liquid B Flow over A Stretching Sheet in a Porous Media, *International Journal of Heat and Mass Transfer*, **127(A)**: 1327-1337 (2018).
- [29] Benos L.Th., Mahabaleshwar U.S., Sakanaka P.H., Sarris I.E., Thermal Analysis of the Unsteady Sheet Stretching Subject to Slip and Magnetohydrodynamic Effects, *Thermal Science and Engineering Progress*, **13**: 100367 (2019).
- [30] Mahabaleshwar, U.S. Sarris I.E., Hill A.A., Lorenzini G., Pop I., An MHD Couple Stress Fluid Due to a Perforated Sheet Undergoing Linear Stretching with Heat Transfer, *International Journal of Heat and Mass Transfer*, **105**: 157-167 (2017).
- [31] Yasuri A.K., Izadi M., Hossein H.M., Numerical Study of Natural Convection in a Square Enclosure Filled by Nanofluid with a Baffle in the Presence of Magnetic Field, *Iran. J. Chem. Chem. Eng. (IJCCE)*, **38(5)**: 209-220 (2019).
- [32] Mohebbi K., Rafee R., Talebi F., Effects of Rib Shapes on Heat Transfer Characteristics of Turbulent Flow of Al₂O₃-Water Nanofluid inside Ribbed Tubes, *Iran. J. Chem. Chem. Eng. (IJCCE)*, **34(3)**: 61-77 (2015).
- [33] Ashraf M.B., Hayat T., Shehzad S.A., Alsaedi A., Mixed Convection Radiative Flow of Three Dimensional Maxwell Fluid over an Inclined Stretching Sheet In Presence Of Thermophoresis and Convective Condition, *AIP Advances*, **5**: 027134 (2015).
- [34] Ashraf M. B., Hayat T., Alsaedi A., Shehzad S.A., Soret and Dufour Effects on the Mixed Convection Flow of an Oldroyd-Bfluid with Convective Boundary Conditions, *Results in Physics*, **6**: 917-924 (2016).
- [35] Turkyilmazoglu M., The Analytical Solution of Mixed Convection Heat Transfer and Fluid Flow of a MHD Viscoelastic Fluid over a Permeable Stretching Surface, *Int. J. Mech. Sci.*, **77**: 263-268 (2013).
- [36] Mabood F., Nayak M.N., Chamkha A.J., Heat Transfer on the Cross Flow of Micropolar Fluids over a Thin Needle Moving in a Parallel Stream Influenced by Binary Chemical Reaction and Arrhenius Activation Energy, *The European Physical Journal Plus*, **134(9)**: 427 (2019).
- [37] Bilal Ashraf M., Hayat T., Alsaedi A., Mixed Convection Flow of Casson Fluid over a Stretching Sheet with Convective Boundary Conditions and Hall Effect, *Boundary Value Problems*, **137**: 2017 (2017).
- [38] Bilal Ashraf M., Hayat T., Alsaedi A., Shehzad S.A., Convective Heat and Mass Transfer in MHD Mixed Convection Flow of Jeffrey Nanofluid over a Radially Stretching Surface with Thermal Radiation, *J. Cent. South Univ.*, **22**: 1114-1123 (2015).
- [39] Sheikholeslami M., Li Z., Shamlooei M., Nanofluid MHD Natural Convection Through a Porous Complex Shaped Cavity Considering Thermal Radiation, *Physics Letters A*, **382**: 1615-1632 (2018).
- [40] Mabood F., Ibrahim S.M., Rashidi M.M., Shadloo M.S., Lorenzini G., Non-Uniform Heat Source/Sink and Soret Effects on MHD Non-Darcian Convective Flow Past a Stretching Sheet in a Micropolar Fluid with Radiation, *Int. J. Heat Mass Transf.*, **93**: 674-682 (2016).